

## The 4-Phenyl-1,2,3,5-dithiadiazole Complex $[\text{Fe}_2(\text{CO})_6(\text{PhCN}_2\text{S}_2)]$ : its Preparation, Crystal Structure, and an Extended-Hückel Molecular-orbital Study of the Bonding †

Arthur J. Banister\* and Ian B. Gorrell

Department of Chemistry, University of Durham, South Road, Durham DH1 3LE

William Clegg

Department of Chemistry, The University, Newcastle upon Tyne NE1 7RU

Karl Anker Jørgensen

Department of Organic Chemistry, Aarhus University, DK-8000 Aarhus C, Denmark

The dithiadiazole  $(\text{PhCN}_2\text{S}_2)_2$  reacts with  $[\text{Fe}_2(\text{CO})_9]$  or  $[\text{Fe}_3(\text{CO})_{12}]$  to give  $[\text{Fe}_2(\text{CO})_6(\text{PhCN}_2\text{S}_2)]$ . The butterfly structure of this complex is similar to that of other  $\text{Fe}_2\text{S}_2$  complexes, with Fe-Fe 2.533(2), S-S 2.930(2), and mean Fe-S 2.225(10) Å. Extended-Hückel molecular-orbital (m.o.) calculations, supported by X-ray structural data, indicate that the unpaired electron (in an antibonding m.o. largely concentrated on the dithiadiazole ligand) is responsible for the very weak S...S and intermolecular N...N interactions.

The 1,2,3,5-dithiadiazoles belong to a remarkable and new class of stable free radicals which are incompletely associated [*e.g.* as dimers  $(\text{PhCNSSN})_2$ ] in the solid state and in solution. For instance, the crystal structure<sup>1</sup> of the phenyl derivative reveals a network of weakly associated dimers, with  $\Delta H$  for dimerisation =  $-35 \pm 2 \text{ kJ mol}^{-1}$ .<sup>2</sup> E.s.r. spectra<sup>2</sup> have shown the presence of free radical monomer in the solid state and in solution.

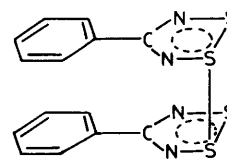
We now report the first transition-metal complex of this novel ligand. Extended-Hückel molecular-orbital calculations and an X-ray crystal structure determination of the bridged complex  $[\text{Fe}_2(\text{CO})_6(\text{PhCN}_2\text{S}_2)]$  indicate that the odd electron remains on the ligand; the shortest intermolecular contacts are between nitrogen atoms and these hold the molecules together in chains.

### Experimental

The carbonyl starting materials were obtained from Strem Chemicals Inc.:  $[\text{Fe}_3(\text{CO})_{12}]$  was used without further purification;  $[\text{Fe}_2(\text{CO})_9]$  was separated from pyrophoric iron by washing with concentrated HCl, distilled water, and finally diethyl ether. The dimer  $(\text{PhCN}_2\text{S}_2)_2$  was prepared from  $[\text{PhCN}_2\text{S}_2]\text{Cl}$  and the Zn-Cu couple<sup>3</sup> except that the pentane extraction was omitted. The salt  $[\text{NO}][\text{BF}_4]$  was obtained from Ventron Alfa Products and was used as supplied.

Toluene was stored for 18 h over  $\text{CaCl}_2$ , refluxed over  $\text{P}_4\text{O}_{10}$ , and then distilled and stored over sodium wire. Dichloromethane was refluxed over  $\text{P}_4\text{O}_{10}$  followed by  $\text{CaH}_2$  and then distilled and stored over molecular sieve (Grade 4A, BDH Ltd.). Tetrahydrofuran was refluxed over potassium then distilled and stored over sodium wire. All distillations were carried out under an atmosphere of dry nitrogen.

Solutions were handled using standard Schlenk techniques and solids were handled in a Vacuum Atmospheres dry-box with an HE493 Dri-Train. Infrared spectra were recorded either as Nujol mulls between KBr plates or as solutions in a  $\text{CaF}_2$



solution cell on either a Perkin-Elmer 577 or a 580B spectrophotometer. Raman spectra were recorded on a Cary 82 instrument, using a Spectra Physics model 164 argon-ion laser at 514.5 nm. Mass spectra were recorded on a VG Analytical 7070E spectrometer using electron impact (e.i.) and chemical ionisation (c.i.) modes. N.m.r. spectra were recorded on a Brüker AC250 spectrometer. Differential scanning calorimetry (d.s.c.) was carried out using a Mettler FP85 thermal analysis cell linked to a Mettler FP80 central processor. Samples were cold sealed in aluminium capsules. The low-temperature bath was regulated using a Haake F3 bath circulator with methylated spirits as coolant.

Sulphur was determined as  $\text{BaSO}_4$  following oxygen-flask combustion. Carbon, hydrogen, and nitrogen were determined by micro-combustion in a Carlo Erba 1106 elemental analyser. Nitrogen was also determined by the micro-Kjeldahl method. Iron was determined using a Perkin-Elmer 5000 atomic absorption spectrophotometer.

**Preparation of  $[\text{Fe}_2(\text{CO})_6(\text{PhCN}_2\text{S}_2)]$ .** From  $[\text{Fe}_2(\text{CO})_9]$ .—The dimer  $(\text{PhCN}_2\text{S}_2)_2$  (0.18 g, 0.5 mmol) and  $[\text{Fe}_2(\text{CO})_9]$  (0.36 g, 1 mmol) were stirred in tetrahydrofuran (thf) ( $25 \text{ m}^3$ ) at  $45^\circ\text{C}$  for 4 h, to give a deep orange-brown solution. The solvent was then pumped off and the solid extracted with toluene ( $4 \times 5 \text{ cm}^3$ ). The residue (0.02 g), a black powder, was insoluble in common organic solvents and was most probably polymeric (Found: Fe, 15.7; N, 2.9; S, 15.3%. Fe:N:S 1.21:0.87:1.00),  $\nu_{\text{max}}$ . 1 150 (sh), 1 110 (sh), 1 050vs, br, and 700w  $\text{cm}^{-1}$  (no CO absorptions). Recrystallisation of the extracted material from toluene gave orange-brown  $[\text{Fe}_2(\text{CO})_6(\text{PhCN}_2\text{S}_2)]$  (0.08 g, 17%), m.p. (from d.s.c.)  $167.2^\circ\text{C}$  followed by decomposition (Found: C, 33.5; H, 1.3; Fe, 24.2; N, 6.0; S, 14.1.  $\text{C}_{13}\text{H}_5\text{Fe}_2\text{N}_2\text{O}_6\text{S}_2$  requires C, 33.8; H, 1.1; Fe, 24.2; N, 6.1; O, 20.8; S, 13.9%).  $\nu_{\text{max}}$ . 2 081vs, 2 070vs, 2 047 (sh), 2 035vs, 2 001vs, 1 988vs, 1 973vs (CO),<sup>4</sup> 1 584vw, 1 533m, 1 522w,

†  $\mu$ -[4-Phenyl-1,2,3,5-dithiadiazolyl- $\text{S}^1(\text{Fe}^{1,2})\text{S}^2(\text{Fe}^{1,2})$ ]-bis(tricarbonyliron) (Fe-Fe).

Supplementary data available: See Instructions for Authors, *J. Chem. Soc., Dalton Trans.*, 1989, Issue 1, pp. xvii-xx.

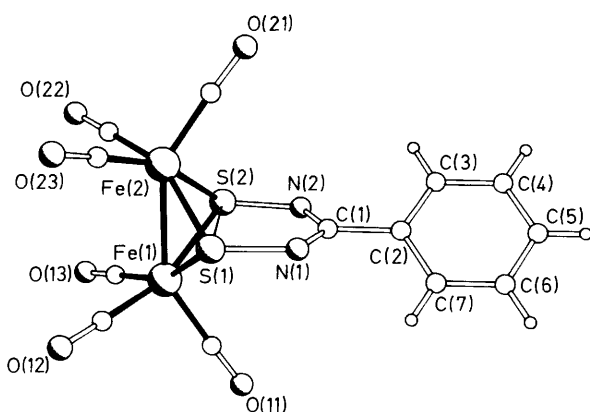
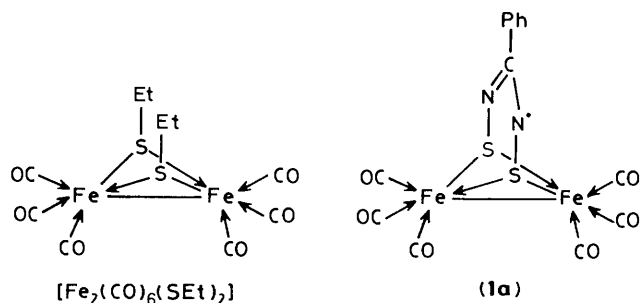


Figure 1. Molecular structure of  $[\text{Fe}_2(\text{CO})_6(\text{PhCN}_2\text{S}_2)]$  with the atom labelling scheme



1 498w, 1 412s, 1 290m, 1 285m, 1 158w, 1 138m, 1 128w, 970vw, 925vw, 906w, 847vw, 764m, 739s, 696s, 677m, 643m, 618s, 602s, 584vs, 563vs, 494m, 461vw, 441w (Nujol); 378s, 224m (Fe-Fe),<sup>5</sup> 180w, 117 (sh), 98s, 61vs, and 43s  $\text{cm}^{-1}$  (Raman).  $\delta_{\text{H}}(\text{CD}_2\text{Cl}_2)$  7.50 (m).  $m/z$  ( $\text{NH}_3$ , negative c.i.) 461 ( $M^+$ , 2), 377 ( $M - 3\text{CO}$ , 85), 349 ( $M - 4\text{CO}$ , 100), 321 ( $M - 5\text{CO}$ , 53), and 293 ( $M - 6\text{CO}$ , 12); ( $\text{NH}_3$ , positive c.i.) 181 ( $\text{PhCN}_2\text{S}_2^+$ , 100), 149 ( $\text{PhCN}_2\text{S}^+$ , 1), 135 ( $\text{PhCNS}^+$ , 8), 117 ( $\text{PhCN}_2^+$ , 0.5), 103 ( $\text{PhCN}^+$ , 53), 77 ( $\text{Ph}^+$ , 52), 64 ( $\text{S}_2^+$ , 2), 46 ( $\text{SN}^+$ , 9) and 32 ( $\text{S}^+$ , 2%). Magnetic measurements were made at 21 °C on a laboratory-built vibrating sample magnetometer. An initial jump in magnetization up to 0.026  $\text{J T}^{-1} \text{kg}^{-1}$  was observed after which the susceptibility (gradient of  $\sigma$  vs.  $B_0$  plot) continued at 0.10  $\text{J T}^{-2} \text{kg}^{-1}$  (between 0.04 and 1.27 T).

From  $[\text{Fe}_3(\text{CO})_{12}]$ . The dimer  $(\text{PhCN}_2\text{S}_2)_2$  (0.18 g, 0.5 mmol) and  $[\text{Fe}_3(\text{CO})_{12}]$  (0.34 g, 0.68 mmol) were stirred in toluene (30  $\text{cm}^3$ ) at 45 °C for 6 h. After allowing to cool at 21 °C, the mixture was filtered to give a brown solid (0.21 g). This was extracted with boiling dichloromethane ( $4 \pm 30 \text{ cm}^3$ ) and recrystallised to give 0.11 g of product. A further 0.06 g was recovered from the filtrate residue and combined with the extracted material to give the total yield of the complex (0.17 g, 37%).  $\nu_{\text{max}}$ . 2 080vs, 2 070vs, 2 048 (sh), 2 036vs, 1 998vs, 1 988vs, 1 978vs (CO), 1 588vw, 1 533w, 1 521w, 1 501w, 1 406m, 1 294m, 1 284m, 1 158w, 1 136w, 1 130w, 1 027vw, 968vw, 929vw, 906w, 851vw, 764m, 738m, 695m, 677w, 647w, 612m, 603m, 581s, 561s, and 493w  $\text{cm}^{-1}$ .  $m/z$  ( $\text{NH}_3$ , negative c.i.) 461 ( $M^+$ , 1), 377 ( $M - 3\text{CO}$ , 2), 349 ( $M - 4\text{CO}$ , 2), 321 ( $M - 5\text{CO}$ , 3), and 293 ( $M - 6\text{CO}$ , 8%).

Crystals of  $[\text{Fe}_2(\text{CO})_6(\text{PhCN}_2\text{S}_2)]$  were grown by cycling the temperature of a saturated dichloromethane solution, immersed in a low-temperature bath, between -10 and 0 °C for 10 d. They were sealed under nitrogen in Lindemann capillaries.

**X-Ray Crystallography.**—Crystal data.  $\text{C}_{13}\text{H}_5\text{Fe}_2\text{N}_2\text{O}_6\text{S}_2$ ,  $M_r = 461.0$ , monoclinic, space group  $P2_1/c$ ,  $a = 13.941(1)$ ,  $b =$

$12.508(1)$ ,  $c = 10.077(1)$  Å,  $\beta = 102.61(1)^\circ$ ,  $U = 1 714.8$  Å<sup>3</sup> (from 2θ values of 24 reflections, 20–25°), Mo- $K_\alpha$  radiation ( $\lambda = 0.710 73$  Å),  $Z = 4$ ,  $D_c = 1.785 \text{ g cm}^{-3}$ ,  $\mu(\text{Mo-}K_\alpha) = 1.96 \text{ mm}^{-1}$ ,  $F(000) = 916$ .

**Data collection and processing.** Siemens AED2 diffractometer, graphite monochromator, crystal size 0.23 × 0.08 × 0.08 mm,  $\omega$ - $\theta$  scan mode, scan width = 0.51° below  $\alpha_1$  to 0.51° above  $\alpha_2$ , scan time = 14–126 s, 2θ 3–50°,  $h$  -16 to 16,  $k$  -14 to 0,  $l$  -11 to 0, no significant variation for three standard reflections, no extinction correction, semiempirical absorption correction (transmission 0.718–0.752); 2 992 reflections measured (all unique), 1 815 with  $F > 4\sigma(F)$ .

**Structure solution and refinement.**<sup>6</sup> Patterson and difference syntheses, blocked-cascade least-squares refinement on  $F$ ,  $w^{-1} = \sigma^2(F)$ , anisotropic thermal parameters, H atoms constrained on ring angle external bisectors with C-H 0.96 Å,  $U(\text{H}) = 1.2U_{\text{eq}}(\text{C})$ , complex neutral atom scattering factors.<sup>7</sup> 226 parameters,  $R = 0.052$ ,  $R' = 0.039$ , slope of normal probability plot = 1.31, maximum/shift/estimated standard deviation, e.s.d.) = 0.014, mean = 0.003, final difference synthesis within  $\pm 0.5e$  Å<sup>-3</sup>.

## Results and Discussion

Reactions of 1,2,3,5-dithiadiazoles  $\text{RCNSSN}^+$  have been largely restricted to facile one-electron oxidations (e.g. with halogens,  $\text{SO}_2\text{Cl}_2$ ,  $\text{SnCl}_4$ , and  $\text{SbCl}_5$ )<sup>3</sup> to give  $\text{RCN}_2\text{S}_2^+$  salts (known since 1977<sup>8</sup>) and to reactions with plasma nitrogen to give  $(\text{PhCN}_2\text{S}_2)_2$ .<sup>9</sup> The most remarkable feature of the dithiadiazoles  $\text{RCNSSN}^+$  is their very low enthalpy of dimerisation (30–35  $\text{kJ mol}^{-1}$ ).<sup>2,10</sup> It is therefore of special interest to prepare complexes and attempt a rationalisation of structures especially where free-radical products are obtained.

The reactions of the dimer  $(\text{PhCNSSN})_2$  with both  $[\text{Fe}_2(\text{CO})_9]$  and  $[\text{Fe}_3(\text{CO})_{12}]$  gave  $[\text{Fe}_2(\text{CO})_6(\text{PhCN}_2\text{S}_2)]$ . Bond lengths and angles are given in Table 1, atomic coordinates in Table 2. The structure (Figure 1), based on the well known  $\text{S}_2$ -bridged di-iron core is, for instance, similar to that of  $[\text{Fe}_2(\text{CO})_6\text{S}_2]$ <sup>11</sup> and  $[\text{Fe}_2(\text{CO})_6(\text{SET})_2]$ .<sup>12</sup> Within experimental error, the Fe-Fe and Fe-S distances are the same in the latter complexes. Since in  $[\text{Fe}_2(\text{CO})_6(\text{SET})_2]$ ,  $d_{\text{SS}} = 2.93$  Å and the sum of the van der Waals radius of sulphur varies between  $\approx 3.2$  Å along the sulphur-sulphur bond and  $\approx 4.0$  Å perpendicular to this bond,<sup>13</sup> there appears to be little or no SS interaction in that complex, or in the aryl derivative  $[\text{Fe}_2(\text{CO})_6(\text{SPh})_2]$ <sup>14</sup> which has an analogous structure ( $d_{\text{SS}} = 2.910$  Å calculated from the atomic co-ordinate). The valence-bond (v.b.) structure (1a) of the new compound appears to be similar to both  $[\text{Fe}_2(\text{CO})_6(\text{SET})_2]$  and  $[\text{Fe}_2(\text{CO})_6(\text{SPh})_2]$ , with SS and SN bond orders of zero and one respectively. The S-S and S-N distances of the ligand have expanded [from 2.089(5) and 1.620(10) Å respectively in  $(\text{PhCN}_2\text{S}_2)_2$ <sup>11</sup>] to 2.930(2) and 1.705(5) Å, (cf.  $d_{\text{SN}} = 1.73$  Å in  $\text{S}_7\text{NH}$ <sup>15</sup>). The other changes in ring parameters, viz.  $\hat{\text{C}} + 6.8$ ,  $\hat{\text{N}} + 9.9$ , and  $\hat{\text{S}} - 13.5^\circ$ , are a natural consequence of the ring expansion at SS and of the loss in NS bond order, which opens up  $\hat{\text{N}}$ .<sup>16</sup>

The presence of short  $\text{N}\cdots\text{N}$  intermolecular contacts (2.84 Å; cf. sum of the van der Waals radii of 3.10 Å<sup>13</sup>) between dithiadiazole units in the crystal (see Figure 2) indicates that the unpaired electron is sited preferentially at nitrogen atoms, as shown (1a). E.s.r. data (isotropic coupling constants) indicate otherwise for the free ligand; in  $\text{PhCNSSN}^+$  the total spin densities are estimated<sup>17</sup> to be in the ratio S:N  $\approx$  6:5. The magnetic properties of  $[\text{Fe}_2(\text{CO})_6(\text{PhCN}_2\text{S}_2)]$ , which will be fully discussed in a future publication, suggest some degree of interaction between magnetic moments.

The primary aims of the extended-Hückel calculations<sup>18</sup>

**Table 1.** Bond lengths (Å) and angles (°) for  $[\text{Fe}_2(\text{CO})_6(\text{PhCN}_2\text{S}_2)]$ 

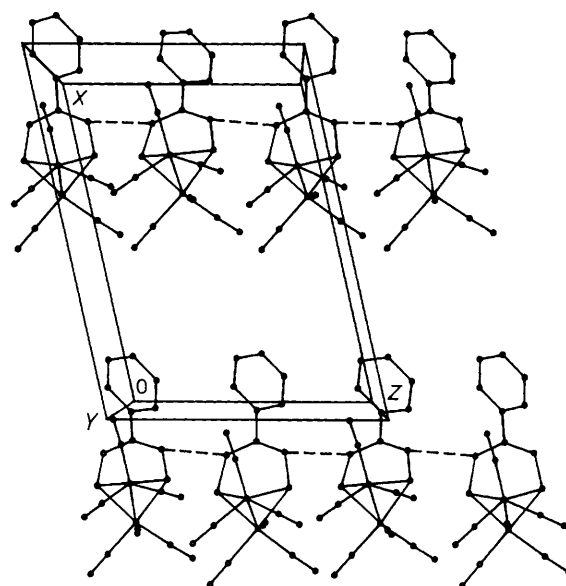
Fe(1)–Fe(2)	2.533(2)	Fe(1)–S(1)	2.232(2)
Fe(1)–S(2)	2.220(2)	Fe(1)–C(11)	1.800(7)
Fe(1)–C(12)	1.786(8)	Fe(1)–C(13)	1.807(6)
Fe(2)–S(1)	2.235(2)	Fe(2)–S(2)	2.211(2)
Fe(2)–C(21)	1.774(7)	Fe(2)–C(22)	1.800(7)
Fe(2)–C(23)	1.805(8)	S(1)–S(2)	2.930(2)
S(1)–N(1)	1.694(5)	S(2)–N(2)	1.716(5)
N(1)–C(1)	1.295(8)	N(2)–C(1)	1.348(7)
C(1)–C(2)	1.494(8)	C(2)–C(3)	1.376(10)
C(2)–C(7)	1.387(9)	C(3)–C(4)	1.387(10)
C(4)–C(5)	1.371(12)	C(5)–C(6)	1.361(13)
C(6)–C(7)	1.366(10)	C(11)–O(11)	1.131(9)
C(12)–O(12)	1.142(10)	C(13)–O(13)	1.126(8)
C(21)–O(21)	1.152(9)	C(22)–O(22)	1.136(9)
C(23)–O(23)	1.137(10)		
Fe(2)–Fe(1)–S(1)	55.5(1)	Fe(2)–Fe(1)–S(2)	55.0(1)
S(1)–Fe(1)–S(2)	82.3(1)	Fe(2)–Fe(1)–C(11)	147.5(2)
S(1)–Fe(1)–C(11)	103.5(2)	S(2)–Fe(1)–C(11)	101.7(2)
Fe(2)–Fe(1)–C(12)	102.6(2)	S(1)–Fe(1)–C(12)	85.3(2)
S(2)–Fe(1)–C(12)	157.5(2)	C(11)–Fe(1)–C(12)	99.4(3)
Fe(2)–Fe(1)–C(13)	102.9(2)	S(1)–Fe(1)–C(13)	157.1(3)
S(2)–Fe(1)–C(13)	91.0(2)	C(11)–Fe(1)–C(13)	99.3(3)
C(12)–Fe(1)–C(13)	93.3(3)	Fe(1)–Fe(2)–S(1)	55.4(1)
Fe(1)–Fe(2)–S(2)	55.3(1)	S(1)–Fe(2)–S(2)	82.4(1)
Fe(1)–Fe(2)–C(21)	146.4(2)	S(1)–Fe(2)–C(21)	106.5(2)
S(2)–Fe(2)–C(21)	97.5(2)	Fe(1)–Fe(2)–C(22)	100.7(2)
S(1)–Fe(2)–C(22)	154.5(3)	S(2)–Fe(2)–C(22)	90.8(3)
C(21)–Fe(2)–C(22)	98.8(3)	Fe(1)–Fe(2)–C(23)	106.7(3)
S(1)–Fe(2)–C(23)	87.5(3)	S(2)–Fe(2)–C(23)	162.0(3)
C(21)–Fe(2)–C(23)	99.7(3)	C(22)–Fe(2)–C(23)	91.9(3)
Fe(1)–S(1)–Fe(2)	69.1(1)	Fe(1)–S(1)–S(2)	48.7(1)
Fe(2)–S(1)–S(2)	48.4(1)	Fe(1)–S(1)–N(1)	113.1(2)
Fe(2)–S(1)–N(1)	114.7(2)	S(2)–S(1)–N(1)	83.0(2)
Fe(1)–S(2)–Fe(2)	69.7(1)	Fe(1)–S(2)–S(1)	49.0(1)
Fe(2)–S(2)–S(1)	49.1(1)	Fe(1)–S(2)–N(2)	111.2(2)
Fe(2)–S(2)–N(2)	109.8(2)	S(1)–S(2)–N(2)	78.3(2)
S(1)–N(1)–C(1)	123.6(4)	S(2)–N(2)–C(1)	127.2(4)
N(1)–C(1)–N(2)	127.8(5)	N(1)–C(1)–C(2)	116.9(5)
N(2)–C(1)–C(2)	115.3(5)	C(1)–C(2)–C(3)	121.8(6)
C(1)–C(2)–C(7)	119.5(6)	C(3)–C(2)–C(7)	118.6(6)
C(2)–C(3)–C(4)	120.0(7)	C(3)–C(4)–C(5)	120.0(8)
C(4)–C(5)–C(6)	120.5(7)	C(5)–C(6)–C(7)	119.7(7)
C(2)–C(7)–C(6)	121.3(7)	Fe(1)–C(11)–O(11)	177.6(7)
Fe(1)–C(12)–O(12)	177.2(6)	Fe(1)–C(13)–O(13)	178.9(7)
Fe(2)–C(21)–O(21)	174.9(6)	Fe(2)–C(22)–O(22)	178.4(7)
Fe(2)–C(23)–O(23)	178.0(7)		

were therefore (i) to rationalise the changes in ligand geometry on co-ordination, (ii) to 'locate' the unpaired electron, and (iii) to check the validity of the simple v.b. bonding description given above.

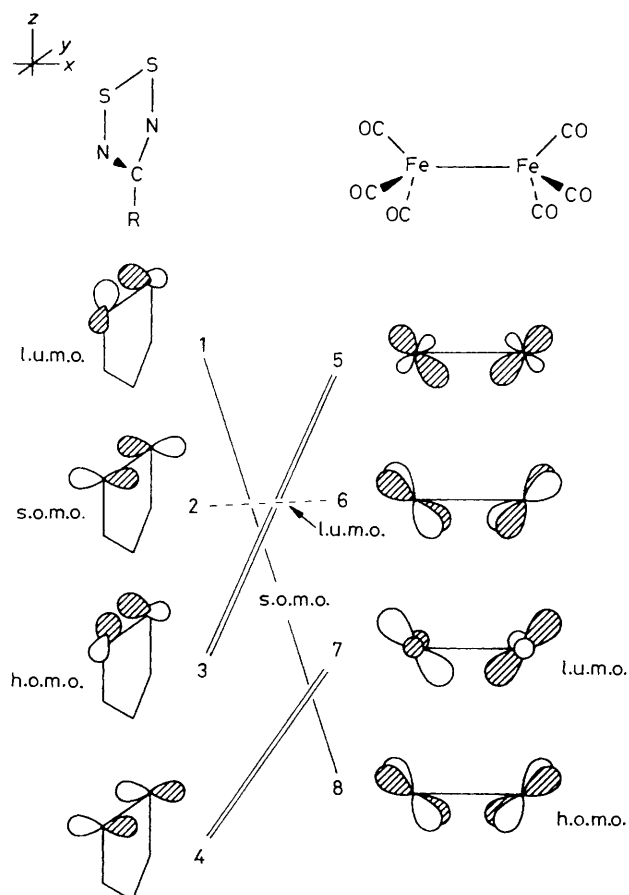
The extended-Hückel model has well known deficiencies and the conclusions drawn here should be viewed, not as a definitive statement, but as an interpretation of bonding trends consistent with the X-ray data and also with several types of calculations that have been reported for analogues  $[\text{Fe}_2(\text{CO})_6\text{S}_2]^{n-}$  ( $n = 0$  or  $2$ )<sup>19–22</sup> and  $[\text{Fe}_2(\text{CO})_6(\text{SMe})_2]$ .<sup>19</sup>

The compound  $[\text{Fe}_2(\text{CO})_6(\text{PhCN}_2\text{S}_2)]$  can be viewed as being constructed of two fragments:  $\text{Fe}_2(\text{CO})_6$ <sup>23</sup> and  $\text{RCN}^-\text{SSN}^+$ . The interaction diagram of these two fragments is rather complex involving much mixing of orbitals; nevertheless the main interactions between the sulphur orbitals on  $\text{RCN}^-\text{SSN}^+$  and the iron orbitals of  $\text{Fe}_2(\text{CO})_6$  can be summarised as in Figure 3.

The frontier orbitals of  $\text{RCN}^-\text{SSN}^+$  are shown as 1–4 with 1 as the lowest unoccupied molecular orbital (l.u.m.o.), 2 the singly occupied molecular orbital (s.o.m.o.), 3 the highest occupied



**Figure 2.** Partial packing view in projection along  $b$ , showing intermolecular  $\text{N} \cdots \text{N}$  interactions forming chains

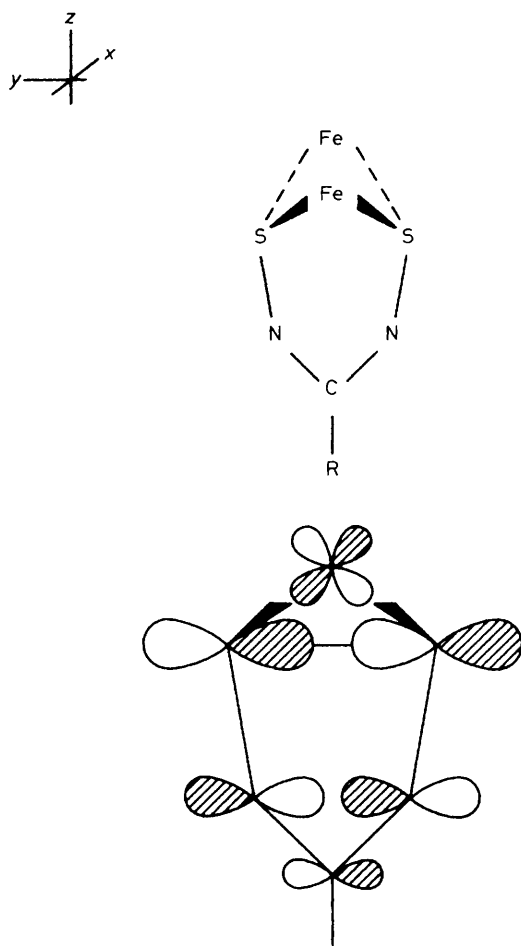
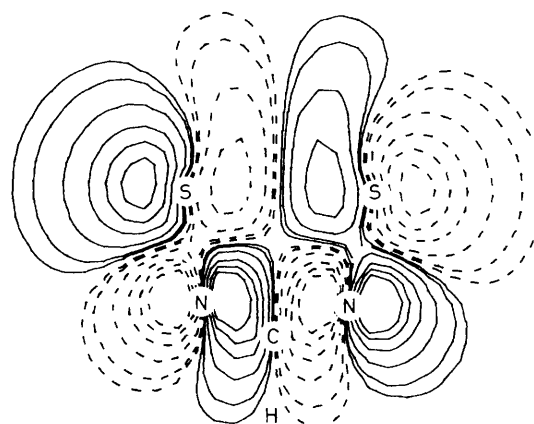


**Figure 3.** Diagrammatic representation of orbitals on the  $\text{PhCN}_2\text{S}_2$  and  $\text{Fe}_2(\text{CO})_6$  components of  $[\text{Fe}_2(\text{CO})_6(\text{PhCN}_2\text{S}_2)]$ . The double lines indicate doubly occupied orbitals in the complex

molecular orbital (h.o.m.o.), and 4 the second h.o.m.o. The frontier orbitals of  $\text{Fe}_2(\text{CO})_6$  which interact with 1–4 are shown as 5–8. The three l.u.m.o.s 5–7 interact with 3, 2, and 4, respectively. The interaction 2/6 produces, after crossing with another orbital, the l.u.m.o. of the complex. The h.o.m.o. of

**Table 2.** Atomic co-ordinates ( $\times 10^4$ )

Atom	x	y	z
Fe(1)	6 373(1)	3 309(1)	4 158(1)
Fe(2)	7 426(1)	4 948(1)	4 075(1)
S(1)	7 652(1)	3 785(1)	5 800(2)
S(2)	7 471(1)	3 477(1)	2 874(1)
N(1)	8 636(3)	2 970(4)	5 911(5)
N(2)	8 521(3)	2 769(4)	3 538(5)
C(1)	8 931(4)	2 606(5)	4 863(5)
C(2)	9 828(4)	1 918(5)	5 137(6)
C(3)	10 550(4)	2 024(6)	4 407(7)
C(4)	11 403(5)	1 421(7)	4 754(8)
C(5)	11 531(6)	727(7)	5 831(8)
C(6)	10 818(6)	610(6)	6 552(8)
C(7)	9 976(5)	1 200(5)	6 211(6)
C(11)	6 320(5)	1 880(5)	4 342(6)
O(11)	6 305(4)	979(4)	4 422(6)
C(12)	5 641(5)	3 703(6)	5 325(8)
O(12)	5 206(4)	3 972(5)	6 103(6)
C(13)	5 376(5)	3 483(6)	2 692(7)
O(13)	4 748(4)	3 600(5)	1 790(5)
C(21)	8 607(5)	5 442(5)	4 004(7)
O(21)	9 377(4)	5 703(5)	3 890(7)
C(22)	6 716(5)	5 620(6)	2 606(8)
O(22)	6 248(4)	6 036(5)	1 687(6)
C(23)	7 083(5)	5 920(6)	5 211(8)
O(23)	6 847(4)	6 511(5)	5 936(6)

**Figure 4.** Diagrammatic representation of the s.o.m.o. (orbital 1–orbital 8 interaction of  $[\text{Fe}_2(\text{CO})_6(\text{PhCN}_2\text{S}_2)]$ )**Figure 5.** Plot of the part of the s.o.m.o. of  $[\text{Fe}_2(\text{CO})_6(\text{PhCN}_2\text{S}_2)]$  located at the dithiadiazole ring. The contour levels of  $\psi$  are 0.1, 0.075, 0.050, 0.025, 0.01, and 0.005. The orbital is plotted in the yz plane

$\text{Fe}_2(\text{CO})_6$ , 8, interacts with 1 and, after crossing other orbitals, leads to an orbital located as the s.o.m.o. of the complex with about 90% contribution from orbital 1. Thus the s.o.m.o. (see Figure 4) is located mainly on the ligand; it contributes slightly to Fe–S and Fe–Fe bonding. There are also lower lying Fe–Fe bonding m.o.s. A contour plot of the dithiadiazole part of the s.o.m.o. is shown in Figure 5. It is particularly interesting that the s.o.m.o. (which is mainly of  $\pi$  character in the ligand plane) is antibonding with respect to both S–S and S–N (*cf.* Figure 4). Consequently, transfer of electron density from orbital 8 into 1 weakens the S–S and the two S–N bonds.

The overall donation of electron density from  $\text{RCN}_2\text{S}_2$  to  $\text{Fe}(\text{CO})_6$  shows up clearly from the net atomic charges on the component fragments: the dithiadiazole unit has an atomic net charge of 0.97 (and the di-iron hexacarbonyl unit  $-0.97$ ).

The antibonding contribution to the S–S and S–N bonds is also apparent from the respective overlap populations. In free  $(\text{RCN}_2\text{S}_2)_2$ , in which the sulphur–sulphur distance is 2.09 Å,<sup>1</sup> the overlap population is 0.52; increasing  $d_{\text{SS}}$  to 2.90 Å reduces the overlap population to 0.36. On co-ordination to  $\text{Fe}_2(\text{CO})_6$ , the sulphur–sulphur overlap population is reduced further to 0.09 and the sulphur–nitrogen overlap population changes similarly on co-ordination from 1.04 in free  $(\text{RCN}_2\text{S}_2)_2$  to 0.85 in the present complex. Significantly, the expanded sulphur–sulphur distance in  $[\text{Fe}_2(\text{CO})_6(\text{PhCN}_2\text{S}_2)]$  strengthens the Fe–S bonding which arises from 1/8 overlap. This rationalises the resistance of the complex to oxidation by  $[\text{NO}][\text{BF}_4]$  (in a 1:1 reaction in  $\text{CH}_2\text{Cl}_2$  at 21 °C for 2 h). The major Fe–S bonding arises from the two highest h.o.m.o.s; there are also two lower-lying m.o.s which are bonding with respect to Fe–S. An increase in  $d_{\text{SS}}$  from 2.09 Å [as in  $(\text{PhCN}_2\text{S}_2)_2$ ] to 2.93 Å (as found for the complex) improves the iron–sulphur overlap from 0.22 to 0.37.

In summary, the complex  $[\text{Fe}_2(\text{CO})_6(\text{PhCN}_2\text{S}_2)]$  (with 18e-iron atoms) is regarded as being essentially composed of one Fe–Fe and four Fe–S bonds, and superimposed upon this skeletal bonding there is back bonding from the h.o.m.o. of  $\text{Fe}_2(\text{CO})_6$  into the l.u.m.o. of  $\text{RCN}_2\text{S}_2$  to produce a s.o.m.o. which is of  $\sigma^*(\text{S–S})$  and  $\pi^*(\text{N–S})$  character. The  $\pi$  acidity of  $\text{RCN}_2\text{S}_2$  is probably the main reason for the marked increase in sulphur–sulphur and sulphur–nitrogen bond lengths on co-ordination. The loss of S–S bonding (due to occupation of the s.o.m.o.) is offset by enhanced Fe–S bonding.

### Appendix

All calculations were performed by using the extended-Hückel model.<sup>18</sup> The orbital parameters along with the  $H_{ij}$  values are summarised in Table 3. The bond lengths and angles used were

**Table 3.** Parameters used in extended-Hückel calculations

Orbital	$H_{ij}/\text{eV}$	Exponent <sup>a</sup> $\zeta_i$
H 1s	-13.6	1.3
C 2s	-21.4	1.55
2p	-11.4	1.325
N 2s	-26.0	1.875
2p	-14.8	1.65
O 2s	-32.3	2.20
2p	-14.8	1.975
S 3s	-20.0	1.967
3p	-13.3	1.517
Fe 4s	-9.1	1.9
4p	-5.32	1.9
3d	-12.60	5.35 (0.536 59) <sup>b</sup>

<sup>a</sup> Coefficients and exponents in a double- $\zeta$  expansion. <sup>b</sup>  $\zeta_2$  1.8 (0.667 79).

as for  $[\text{Fe}_2(\text{CO})_6(\text{PhCN}_2\text{S}_2)]$  (X-ray data) but with the exchange of the phenyl group by hydrogen.

### Acknowledgements

We thank Professor Roald Hoffmann for his helpful comments, the S.E.R.C. for research grants to A. J. B. and to W. C. (for crystallographic equipment), and Mr. R. Coult and Dr. D. B. Lambrick, the University of Durham, for analyses and the magnetisation measurements respectively.

### References

- 1 A. Vegas, A. Pérez-Salazar, A. J. Banister, and R. G. Hey, *J. Chem. Soc., Dalton Trans.*, 1980, 1812.
- 2 S. A. Fairhurst, K. M. Johnson, L. H. Sutcliffe, K. F. Preston, A. J. Banister, Z. V. Hauptman, and J. Passmore, *J. Chem. Soc., Dalton Trans.*, 1986, 1465.

- 3 A. J. Banister, N. R. M. Smith, and R. G. Hey, *J. Chem. Soc., Perkin Trans. 1*, 1983, 1181.
- 4 J. A. De Beer and R. J. Haines, *J. Organomet. Chem.*, 1970, **24**, 757.
- 5 W. M. Scovell and T. G. Spiro, *Inorg. Chem.*, 1974, **13**, 304.
- 6 G. M. Sheldrick, SHELXTL, an integrated system for solving, refining, and displaying crystal structures from diffraction data, University of Göttingen, 1978.
- 7 'International Tables for X-Ray Crystallography,' Kynoch Press, Birmingham, 1974, vol. 4, pp. 99, 149.
- 8 G. G. Alange, A. J. Banister, B. Bell, and P. W. Millen, *Inorg. Nucl. Chem. Lett.*, 1977, **13**, 143.
- 9 A. J. Banister, M. I. Hansford, and Z. V. Hauptman, *J. Chem. Soc., Chem. Commun.*, 1987, 63.
- 10 N. Burford, J. Passmore, and J. C. P. Sanders, in 'Molecular Structure and Energetics,' vol. 8, eds. J. F. Liebman and A. Greenberg, V.C.H. Publishers Inc., New York, 1988, in the press; W. V. F. Brooks, N. Burford, J. Passmore, M. J. Schriver, and L. H. Sutcliffe, *J. Chem. Soc., Chem. Commun.*, 1987, 69.
- 11 C. H. Wei and L. F. Dahl, *Inorg. Chem.*, 1965, **4**, 1.
- 12 L. F. Dahl and C-H. Wei, *Inorg. Chem.*, 1963, **2**, 328.
- 13 S. C. Nyburg and C. H. Faerman, *Acta Crystallogr., Sect. B*, 1985, **41**, 274.
- 14 W. Henslee and R. E. Davis, *Cryst. Struct. Commun.*, 1972, **1**, 403.
- 15 J. Weiss and H-S. Neubert, *Acta Crystallogr.*, 1965, **18**, 815.
- 16 A. J. Banister, I. B. Gorrell, and R. S. Roberts, *J. Chem. Soc., Faraday Trans. 2*, 1985, 1771.
- 17 L. H. Sutcliffe, personal communication.
- 18 R. Hoffmann, *J. Chem. Phys.*, 1963, **39**, 1397; R. Hoffmann and W. L. Lipscomb, *ibid.*, 1962, **36**, 2179.
- 19 B. K. Teo, M. B. Hall, R. F. Fenske, and L. F. Dahl, *Inorg. Chem.*, 1974, **14**, 3103.
- 20 E. L. Andersen, T. P. Fehlner, A. E. Foti, and D. R. Salahub, *J. Am. Chem. Soc.*, 1980, **102**, 7422.
- 21 R. L. DeKock, E. J. Baerends, and A. Oskam, *Inorg. Chem.*, 1983, **22**, 4158.
- 22 R. L. DeKock, E. J. Baerends, and R. Hengelmolen, *Organometallics*, 1984, **3**, 289.
- 23 D. L. Thorn and R. Hoffmann, *Inorg. Chem.*, 1978, **17**, 126.

Received 22nd July 1988; Paper 8/03020K